$D_2 8 - 46$

18912

N87-10447

3.2.7 COMPARISON BETWEEN S.T. RADAR AND IN SITU BALLOON MEASUREMENTS

F. Dalaudier[1], J. Barat[1], F. Bertin[2], E. Brun[3],
M. Crochet[3], and F. Cuq[3]

[1]Service d'Aeronomie du CNRS, BP3-91370 Verrieres-le Buisson, France
[2]CNET/CRPE 4 Avenue de Neptune 94107, St Maur des Fosses, France
[3]LSEET UA 705, Universite de Toulon, France

A campaign for simultaneous in situ and remote observation of both troposphere and stratosphere took place near Aire-sur-l'Adour (in southeastern France) on May 4, 1984. The aim of this campaign was a better understanding of the physics of radar echoes. The backscattered signal obtained with an ST radar both at the vertical and 15° off vertical is compared with the velocity and temperature measurements made in the same region (about 10 km north of the radar site) by balloon-borne ionic anemometers and temperature sensors.

Radar Description	Balloon Characteristics
Frequency: 47.8 MHz (λ = 6.3 m)	Diameter: 20 m
Antenna: coaxial collinear, 2560 m^2	Ascending velocity: 3 to 5 m/s
Beamwidth: 8.8°	Ionic anemometer, accuracy: 0.02 m/s
Range resolutions: 300, 750, 2400 m	Temperature sensor, accuracy: 0.01 K
Duty cycle: 0.5 to 1%	Balloon trajectory: given in Figure 1

The detailed analysis of the results obtained is not yet achieved. We present here some preliminary results.

1. RADAR RESULTS

Typical examples of radar power return are given in Figure 2, in oblique (Figure 2a) and vertical (Figure 2b) directions. The vertical line at −10 dB corresponds to the limit of detectability. The signal-to-noise ratio is 5 to 10 dB stronger in the vertical than in the oblique direction. An enhancement of the radar power return is observed in the lower stratosphere both in oblique and vertical directions, but in the latter direction, the enhancement is affected by a temporal variability.

2. BALLOON RESULTS

A comparison between velocity and temperature variance profiles is given in Figure 3 and suggests the following comments:
- As a general rule, the velocity variance is much smaller in the stratosphere than in the troposphere because of the hydrostatic stability in the former. On the other hand, temperature variance is far greater in the stratosphere than in the troposphere. This is the consequence of the atmospheric stratification.
- Six turbulent layers (labelled from 1 to 6 in Figure 3) are clearly observed both in velocity and temperature profiles.
- In the stratosphere, maxima in temperature variance are not always associated with maxima in velocity variance. In these regions, the temperature fluctuations are not compatible with the classical turbulence theory, although they contribute to the radar power return.

The temperature gradient profile obtained from the balloon-borne temperature sensors (Figure 4a) exhibits a rather complex structure in the stratosphere: very strong gradients may arise in very thin layers (few meters width). The horizontal extent of these thin layers is not known but, as a general rule, it is observed (Figure 4b) that in regions where the mean
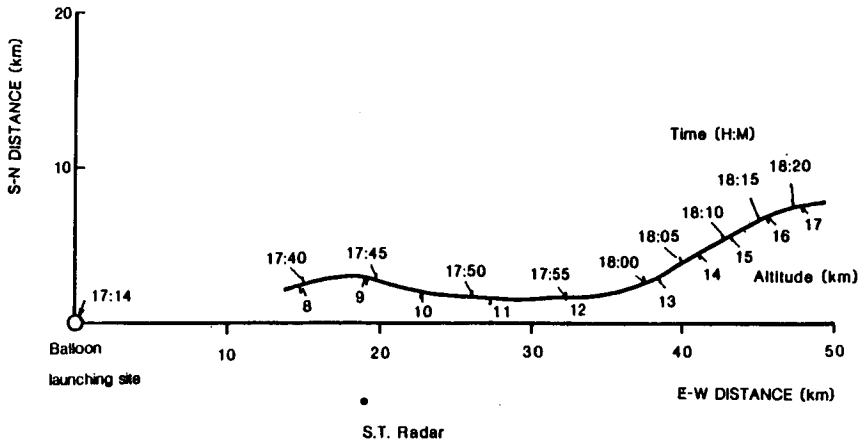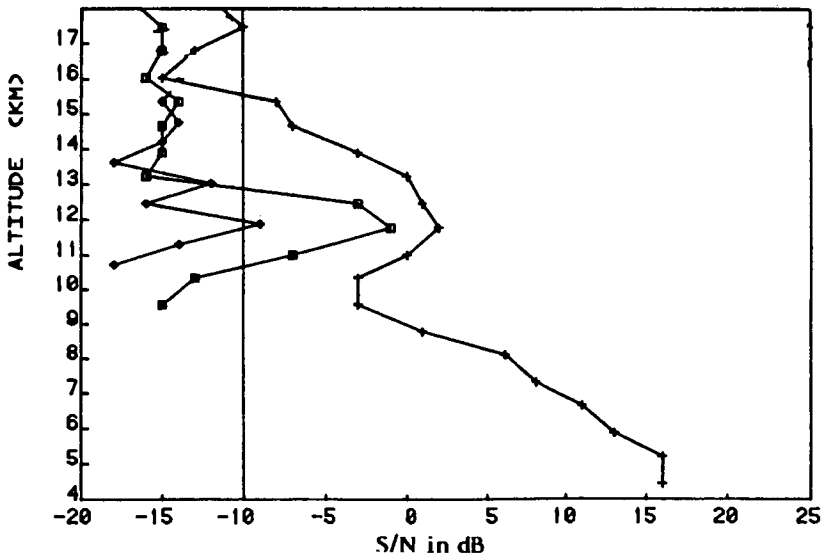
Figure 1. Balloon trajectory.

Figure 2a. Radar power return obtained in oblique direction
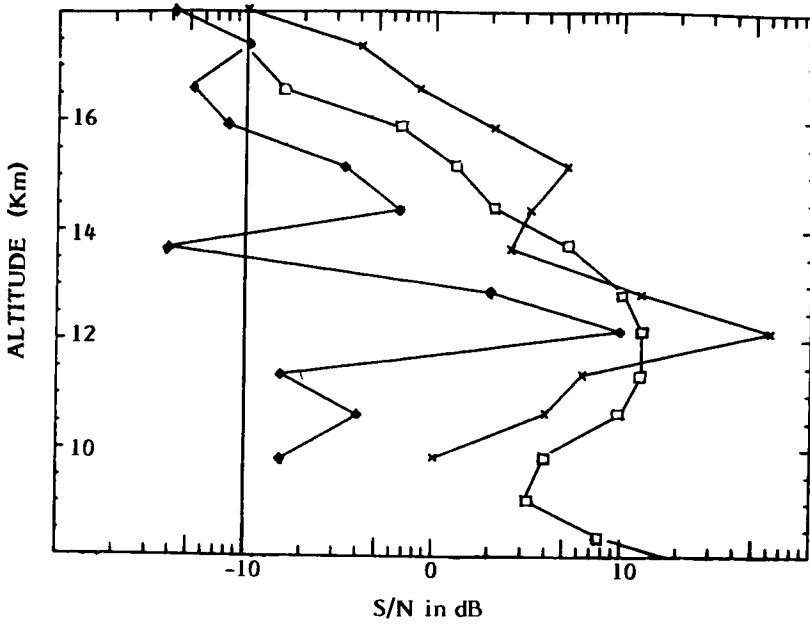for three range resolution: 2400 m (++), 750 m (□□), and
300 m (◆).

Figure 2b.   Radar power return obtained at the vertical for three range resolutions: 2400 m (□□), 750 m (××), and 300 m (◆).
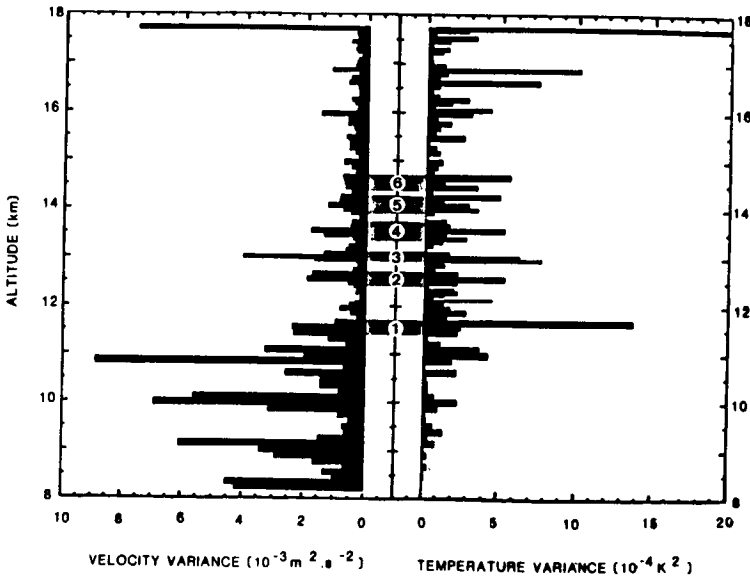

Figure 3.   Comparison between velocity and temperature variances.   Six turbulent layers are observed.
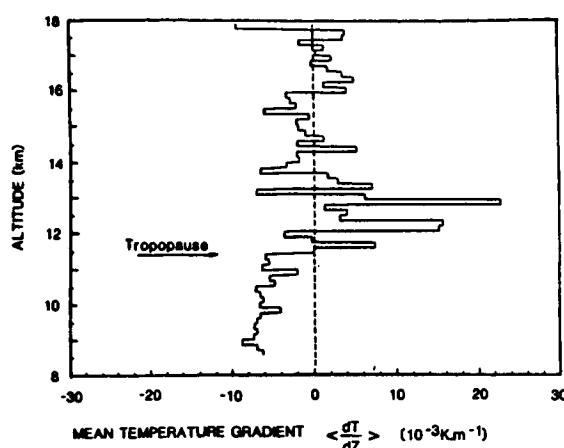
Figure 4a. Mean temperature
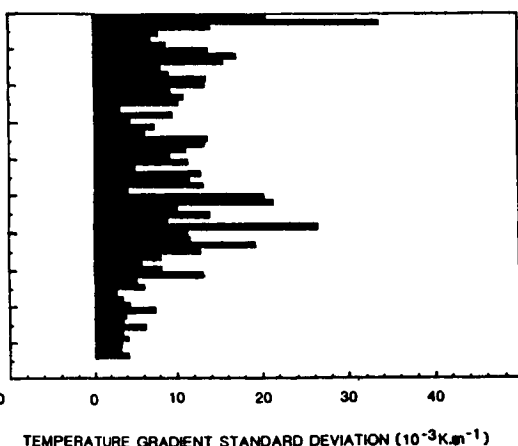   gradient (over 150 m)
    profile.

Figure 4b. Temperature gradient
    standard deviation (over
    150 m).

gradient (over 150 m) is highly positive, the standard deviation of the local
gradients is important, its value being of the same order as the mean gradient
itself.

3. COMPARISON BETWEEN RADAR BALLOON RESULTS

3.1 Oblique direction. The theoretical radar reflectivity $\eta(k)$ and the
C_n^2 parameter have been estimated (under the classical quasi-isotropy
assumption) from the temperature fluctuation spectra computed in successive 30-
m width layers. The amplitude of the spectra for the value $k_o = 4\pi/\lambda$ gives,
after integration through the appropriate radar weighting function, an
estimation of (k) and C_n^2. The following expressions (OTTERSTEN 1969) are
used:

$$\eta(k) = 5/3 \ (\pi/8) \ k_o S_n(k)$$

$$\eta(k) = 0.38 \ C_n^2 \lambda^{-1/3}$$

In (1), $S_n(k_o)$ is the normalized one-dimensional spectrum of turbulence,
while in equation (2), a k spectrum is assumed.

The $\eta(k)$ profile so obtained is compared in Figure 5 with the radar
results. For this comparison, the $\eta(k)$ values calculated from balloon
measurements are systematically divided by ten. It can be seen on this figure
that radar and balloon $\eta(k)$ profiles exhibit a remarkably similar shape. This
good general agreement confirms that the radar echo power is strongly
correlated with the amplitude of the temperature fluctuation spectra. However,
as shown in Section 2, the assumption used in equations (1) and (2), (isotropy
of the turbulent field and spectra in $k^{-5/3}$) for calculating the radar
reflectivity, are certainly not always fulfilled. This discrepancy with
respect to the classical theory may explain the systematic difference between
the η values respectively calculated from radar and balloon-borne measurements.

In fact, the one-dimensional spectrum $S_n(k)$ of temperature fluctuations
along the balloon trajectory is an integral in the Fourier space and in a plane
perpendicular to the k_o vector. Note that all these contributions are coming
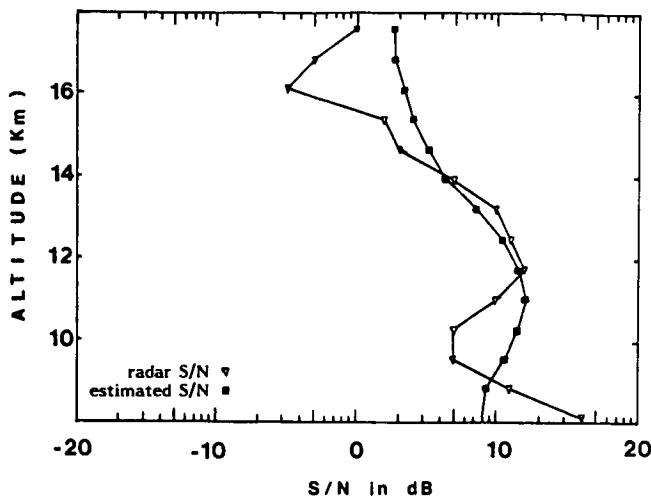
Figure 5. Comparison between oblique
power return of the radar and in
situ estimation of radar reflec-
tivity from equation 1.

from k vectors greater or equal to k_o. On the other hand, the radar samples
the three-dimensional spectrum $\phi(k)$ at the particular mode k_o in the radar
radial direction. So, the observed difference between radar and balloon
estimation of $\eta(k)$ could be the consequence of the three-dimensional spectrum
anisotropy for k values greater than k_o i.e., for wavelength $\lambda < 3$ m. However,
this assumed small-scale anisotropy is in contradiction with turbulent fields
generally observed that appear to be quasi-isotropic for scales smaller than
10 m (BARAT and BERTIN, 1984). Consequently, the above assumed small-scale
anisotropy could be associated with the nonturbulent fine structure of the
temperature profiles observed in stratified fluids. This hypothesis is
supported by the balloon observation of strong increase of the temperature
gradient variance in highly stratified regions (see Figure 4b).

3.2 Vertical direction. The observed radar signal is 5 to 10 dB stronger
at the vertical than in the oblique direction but is affected by a greater
variability. The intensification of the echo power at the vertical is
generally interpreted as the result of a partial reflection on stable layers in
the stratosphere. The particular thermal structure of the stratosphere
observed in Figure 4a and 4b may explain the two main characteristics of the
vertical radar return power profile:
 - spatial stability of the enhanced echoes which occur in regions where
the mean temperature gradient exhibits maxima
 - temporal variability of these enhancements which could be explained by a
limited spatial extent of the thin layers where the strongest gradients occur.
An estimation of the radar reflection coefficient (GAGE and BALSLEY, 1980)
computed from the temperature gradient profile is given in Figure 6. In this
estimation, the contribution of the individual layers have been incoherently
added in the radar resolution range. The shape of this profile is in general
agreement with the radar vertical profiles of signal-over-noise ratio. This
result, obtained with simultaneous measurements, confirms the strong correla-
tion between mean stratification and strengthening of radar vertical echo power
already mentioned by GREEN et al. (1980). Moreover, the detailed temperature
profile shows that these regions of strong stratification are also regions of
highly layered temperature gradient (see Figure 4b), leading to an increase of
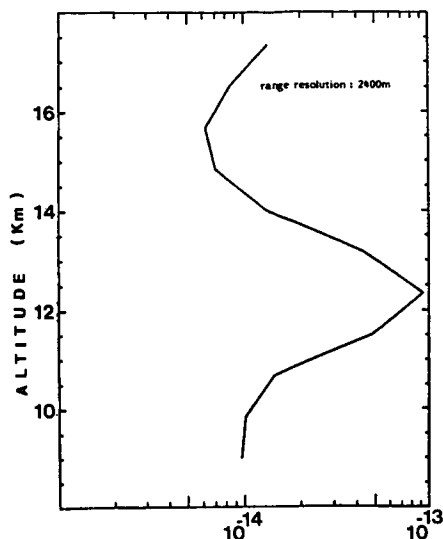reflection coefficient in the vertical direction.

Figure 6. Estimation of the radar vertical reflection coefficient from the temperature gradient profile.

CONCLUSION

In situ measurements clearly indicate that the temperature fluctuations are not always consistent with the standard turbulent theory. Nevertheless, the assumptions generally made (isotropy and turbulent field in k) and the classical formulation so derived for radar reflectivity (equations 1 and 2) are able to reproduce the shape of the radar return power profiles in oblique directions. Another significant result is the confirmation of the role played by the atmospheric stratification in the vertical echo power. It is important to develop these simultaneous in situ and remote experiments for a better description of the dynamical and thermal structure of the atmosphere and for a better understanding of the mechanisms governing clear-air radar reflectivity.

REFERENCES

Barat, J., and F. Bertin (1984), Simultaneous measurements of temperature and velocity fluctuations within clear air turbulence layers: analysis of the estimate of dissipation rate by remote sensing techniques, J. Atmos. Sci., 41, 1613.

Gage, K. S., and B. B. Balsley (1980), On the scattering and reflection mechanisms contributing to clear air echoes from troposphere and stratosphere, Radio Sci., 15, 243.

Green, J. L., and K. S. Gage (1980), Observation of stable layers in the troposphere and stratosphere using VHF radars, Radio Sci. 15, 399.

Ottersten H. (1969), Atmospheric structure and radar backscattering in clear air, Radio Sci. 4, 1179.